

Measurements of photon scattering lengths in scintillator and a test of the linearity of light yield as a function of electron energy

Alexandra Huss

August 31, 2013

Abstract

The SNO+ experiment in Sudbury, Canada will utilize approximately 800 tons of liquid scintillator in an attempt to detect neutrinoless double beta decay and measure solar neutrinos and geoneutrinos. The type of particle that interacted with the scintillator yields information about the emitted time spectrum of photons. The ability to detect this time dependency may depend on the scattering length of the photon because a photon's path to a light detector is less predictable if its scattering length is short compared to the distance it traveled before detection. In order to determine the energy of an interacting particle, it is also necessary to determine the relationship between light yield and energy. This relationship is tested by measuring the light output of electrons at very low light intensities. It is found that there is a change in linearity for electron energies at 0.4MeV. I will discuss the measurements made to test the linearity of light yield versus electron energy and measurements made to determine the scattering length of photons in scintillator samples.

1 Introduction

SNO+ is a neutrino experiment that will be able to detect neutrinoless double beta decay, low energy solar neutrinos, geoneutrinos and supernova neutrinos using scintillation [1]. Located approximately 2km underground at the SNOLAB facility in Sudbury, Ontario, Canada, it is a detector that will be filled with roughly 780 tons of liquid scintillator. The scintillator used will be Linear Alkyl Benzene (LAB) that will be contained in an acrylic vessel 12m in diameter, and surrounded by approximately 9500 PMTs. For detections of neutrinoless double beta decay, the liquid scintillator will be loaded with 0.1% Nd by

weight, corresponding to about 44kg of Nd for the entire scintillator [2].

To obtain results in this experiment, certain properties of the scintillator must be understood, particularly the scattering length of photons in the scintillator and the dependence of light yield on electron energy. The scattering length is the distance a photon will travel before its path is redirected, and this length has a different value in different materials. Neutrinos are detected by looking at the time spectrum of photons that are detected by PMTs. This spectrum is used to trace the photon path back to a scintillation event. If the scattering length of the photon is less than the diameter of the scintillator, photons will not

travel the expected direct path to PMTs. In this case, the time spectrum of PMT detection is less predictable, and detection of neutrinos is much more difficult. The aim of this work is to calculate the scattering length of photons in different scintillator samples to determine which dopant material gives a long enough scattering length to maintain a predictable time spectrum of photon detection, and therefore detection of neutrinos.

The dependence of light yield on electron energy must be understood in order to understand the properties of the scintillator down to the SNO+ energy threshold, about 0.2MeV. In scintillators, this dependence is typically linear, except at low energies. Previous experiment has shown that in scintillator, the linearity of the relationship changes at approximately 0.4MeV [3]. This work aims to test this linearity at very low light intensities in order to establish a single photon scale for light yield that can be used to calibrate light yield at higher energies, and remove the arbitrary units of light yield used in previous experiments.

2 Scattering

2.1 Motivation

In the SNO+ experiment, neutrinos are detected using a time spectrum event traceback: the neutrinos interact with electrons and nuclei in the detector to produce a charged particle, which when passing through the scintillator, emits light. The emitted light is detected by PMTs surrounding the scintillator, and the time of detection of the photons for all of the PMTs is combined, creating a detection time spectrum. This spectrum is used to trace the emitted light back to the scintillation event,

giving information about the location of the neutrino that caused the event.

If a photon scatters before reaching the predicted PMT, the detection time spectrum cannot be composed properly and the detection of neutrinos becomes very difficult. Thus, an ideal dopant in the scintillator would give a scattering length that is greater than the diameter of the scintillator. Rayleigh scattering, which occurs for particles small compared to the wavelength of incident light, is the approximation used to determine the scattering length of photons in scintillator samples. It is a result of the electric polarizability of particles [4], and the intensity of Rayleigh-scattered light is given by

$$I = \frac{I_0 \alpha}{\lambda^4} (1 + \cos^2 \theta) \quad (1)$$

where α is a combination of constants, and the $1 + \cos^2$ term corresponds to the light polarization, to be explained in further detail in Section 2.2. The dependence of the intensity of scattered light on wavelength, angle, and input and output polarization calls for data collection at a variety of wavelengths, angles, and polarizations in order to determine the scattering length of photons in scintillator.

2.2 Method

The apparatus used to collect data for scattering measurements is shown in Figure 1.

The setup is housed in a dark box, and includes a laser, filters, scintillator sample, two PMTs, and a baffle. The laser beam, which can be interchanged for different laser wavelengths, is aligned so that the beam is incident on the scintillator sample in the center of the dark box. The “normalizing” PMT is mounted to the table on the other side of the box, and is used to

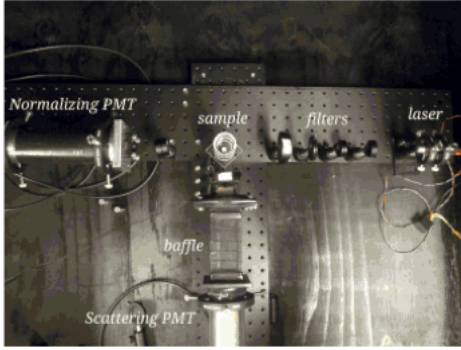


Figure 1: A photo of the scattering apparatus, housed in a dark box. To the right is the laser that is incident on the filters and scintillator sample. The normalizing PMT is shown to the left, and the scattering PMT at the bottom, with the baffle in front of it.

measure the total amount of laser light that passes through the sample. The "scattering" PMT is used to measure the amount of light that scatters from the scintillator, and is free to be repositioned so that scattering measurements can be taken at a variety of angles. The baffle placed in front of the scattering PMT is designed to only accept light that has scattered near the axis of the sample holder, and in front of that is an adjustable polarizing filter to select either vertical or horizontal polarizations of outgoing light. The table also has space to insert additional filters, which are used to remove unwanted harmonics from frequency doubled lasers, adjust light intensity, constrict laser beam size, and select horizontal or vertical incident polarization.

Measurements of normalized and scattered light are made at wavelengths of 405, 447, 473, 532, and 650nm. For each wavelength, measurements are taken at all possible combinations of angles of 45, 60, 75, and 90 degrees and polarizations (VV, VH, HH, HV, corresponding to vertical or horizontal polarizations of incident and scat-

tered light). For each measurement, dark rates are also recorded by placing an absorbing beam block in front of the scintillator sample. By doing this, light that bounces off of the walls of the box as well as the internal dark rate of the PMTs can be subtracted from the scattering counts.

PMT counts are recorded for both the normalizing and scattering PMTs by an ADC output to which they are connected. The resulting counts are recorded in an excel spreadsheet and imported into ROOT. A series of calculations must first be carried out before the data is fit to the Rayleigh scattering function and are described below.

First, there is a dead time correction that takes into account the $7.5\mu\text{s}$ dead time of the ADC output that follows each count. The dead time correction, described by

$$r = \frac{m}{1 - md} \quad (2)$$

is applied to both the normalization and scattering counts, where m is the measured number of counts, d is the dead time of $7.5\mu\text{s}$, and r is the corrected number of counts. The appropriate dark rates are subtracted from the corrected normalized and scattering counts, and the resulting scattering counts are divided by the normalized counts to remove dependence on absolute laser brightness. There is also a filter correction that is based on the published transmissivities of filters at specific wavelengths: for each individual filter used at a specific wavelength, the scattering or normalized counts are corrected accordingly. Finally, there is a geometric correction that is applied based on the setup of the apparatus: all types of scattering is scaled by a factor of $\sin(\theta)^{-1}$, and is therefore corrected by multiplying all scattering measurements by $\sin(\theta)$, where θ is the

scattering angle.

The corrected data is then fit to the following equations:

$$VV = \frac{R}{\lambda^4} + A(\lambda) \quad (3)$$

$$VH = A(\lambda) \quad (4)$$

$$HH = \frac{R \cos^2 \theta}{\lambda^4} + A(\lambda) \quad (5)$$

$$HV = A(\lambda) \quad (6)$$

where “R” designates Rayleigh scattering, and $A(\lambda)$ is an absorption-reemission term. As shown by the equations, there is no Rayleigh scattering term for cross-polarizations, but for vertically polarized input and output polarizations (“VV”), there is equal scattering in all directions, and for horizontally polarized input and output polarizations (“HH”), there is a $\cos^2 \theta$ distribution of the scattering, where θ is the angle between incident and scattered light. The Rayleigh dependence is a result of the electric field components: for VV, the incoming and outgoing components are always parallel, but the incoming and outgoing components for HH vary with angle, following a \cos^2 distribution. The term $A(\lambda)$ is independent of polarization, but does have an unknown wavelength dependence.

With optimized parameters for Rayleigh scattering and absorption-reemission, and allowing for background scattering, the data is fit to these equations, and the results of the fit are used to determine the scattering length of photons in the scintillator sample.

2.3 Results

The fit results for a sample of Nd 0.3%, using a 405nm laser plotted as a function of angle are shown in Figure 2. The shape

of the fit corresponds to equations 3, 4, 5, and 6 as expected: the cross polarizations do not have Rayleigh scattering components, the vertical-vertical polarization has the greatest amount of Rayleigh scattering and is approximately equal for all angles, and the horizontal-horizontal polarization changes as a function of angle, where at 45 degrees it is approximately half that of the vertically-vertically polarized light.

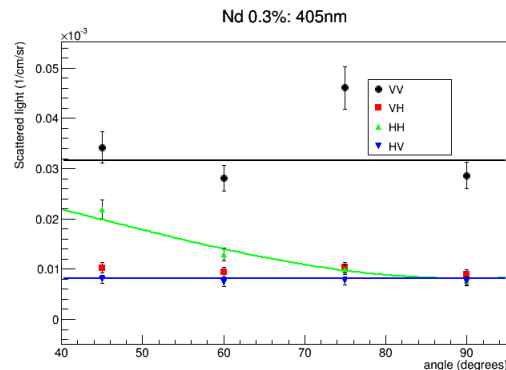


Figure 2: Rayleigh scattering fit results for scintillator doped with Nd 0.3% at 405nm, plotted as a function of angle. Black circles are data points for VV polarization, green triangles are data points for HH polarization, red squares are data points for VH polarization, and blue triangles are data points for HV polarization, each with a corresponding fit line.

The optimized parameters of the fit function are used to calculate the scattering length of photons in the scintillator. To do this, one integrates over the solid angle, averages over the incident polarization (because only half of the incident photons will have each polarization), sums over the scattered polarizations (because a photon could scatter with either polarization, but all scattering needs to be included), and finally inverts. This calculation is described by equation 7 where s.f. is scattering fraction:

$$\text{scattering length} = \frac{1}{\int (s.f.d\Omega)} \quad (7)$$

The results of the scattering length calculations for samples of Nd .03%, Nd 0.3% +BisMSB, and Te 0.3% +BisMSB for all five wavelengths are reported in Table 1.

Table 1: *Scattering length results*

Sample	405nm	447nm	473nm	532nm	650nm
Nd 0.3%	25.46m	37.79m	47.38m	75.82m	168.96m
Nd 0.3% +BisMSB	19.66m	29.18m	36.59m	58.54m	130.47m
Te 0.3% +BisMSB	4.28m	6.35m	7.97m	12.75m	28.41m

2.4 Discussion

The scattering results show that Nd doped scintillator samples have a longer scattering length than Te doped samples. For each of the five wavelengths, both Nd 0.3% and Nd 0.3% +BisMSB have scattering lengths much longer than the diameter of the scintillator. If these dopants were used in the scintillator for SNO+, the neutrino detection process would be well understood because the time spectrum of photons detected by PMTs is predictable. For the Te doped sample however, the scattering length for the 405, 447 and 473nm lasers was shorter than the diameter of the sample, which would make neutrino detection much more difficult because the origin of the scintillation cannot be directly traced back in the scintillator. Therefore, Nd is a more ideal dopant for the scintillator in the SNO+ experiment.

It is important to consider how well the Rayleigh function actually fits the data. When plotted as a function of wavelength at a specific angle, as shown in Figure 3, the Rayleigh function does not fit as well as expected, where the fit lines do not reach

the data. Therefore, the possibility that Rayleigh scattering is not the scattering occurring in the sample must be considered. The size of the particle may be slightly larger than expected, placing the scattering type out of the Rayleigh regime and into the Mie scattering regime, where particles are more than one-tenth the size of the wavelength. In Mie scattering, more forward scattering is expected than back scattering, therefore it may provide a better fit to the data. Mie scattering will therefore be examined; scattering lengths will be recalculated based on Mie optimized fits and will be compared to the Rayleigh scattering fit.

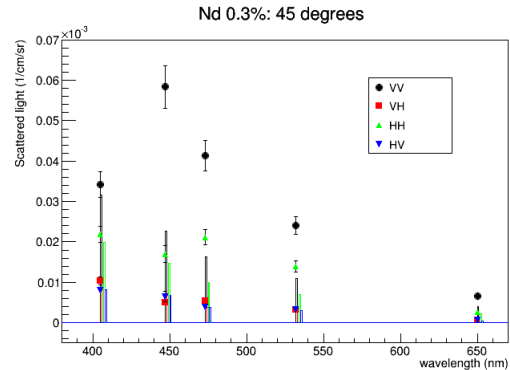


Figure 3: *Rayleigh scattering fit results for scintillator doped with Nd 0.3% at 45 degrees, plotted as a function of wavelength. The Rayleigh fit does not fit the data well, therefore the possibility of Mie scattering will be considered.*

3 Light Yield as a Function of Energy

3.1 Method

To conduct the SNO+ experiment, it is necessary to understand the properties of the scintillator down to the SNO+ energy

threshold, approximately 0.2MeV. Therefore, it is also necessary to understand the dependence of light yield on electron energy: this relationship is usually linear except at low energies, where at approximately 0.4MeV, there is a change in linearity. Reference [3] verified the value of 0.4MeV, although the use of ADC counts as an arbitrary unit for light yield in that experiment can be rectified by looking at the light yield versus energy relationship at very low light intensities, specifically single photons. The photon can then be used as a base unit to calibrate light yield at higher intensities.

In order to collect data at such low light intensities, the apparatus shown in Figure 4 was used. An electronics chain consisting of a preamplifier, amplifier, delay module, and second amplifier is not shown, but is used to trigger the ADC output on LED pulses so that pulses are less likely to be missed during an ADC dead time. The apparatus shown is housed in a dark box, and the light emitting diode (LED) driver circuit is connected to a function generator (not shown) running at a frequency of 10kHz. The LED driver circuit is wired so that its outputs, which are connected to the LED circuit that holds two LEDs, will pulse in a pattern such that LED1 lights up, LED2 lights up, then both LEDs light up together. The PMT detects the light output of the LEDs, and is connected to an ADC output that collects the number of counts. The LED driver circuit also has inputs from a power source (not shown), so that very low light intensities can be reached and the voltage can be varied for each of the LEDs separately.

Once the data is collected, it is then fit to a function that multiplies the Gaussian and Poisson distributions. The Gaussian distri-

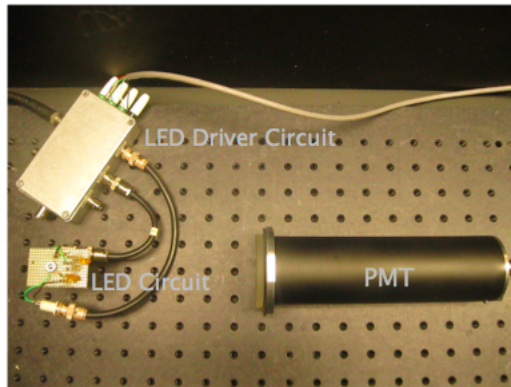


Figure 4: Apparatus consisting of an LED driver circuit, LED circuit, and PMT, used to count light yield at very low intensities.

bution, given by equation 8, is used because it describes the shape of the single photon peak, and a Poisson distribution, given by equation 9, describes the detection of the photons, where λ is the expected number of events and k is the number of detected photons [5].

$$P(x) = \frac{e^{-\frac{(x-\mu)^2}{(2\sigma)^2}}}{\sigma\sqrt{2\pi}} \quad (8)$$

$$P(k; \lambda) = \frac{\lambda^k e^{-\lambda}}{k!} \quad (9)$$

The results of this fit with LED1 powered by 6.8V and LED2 powered by 6.5V are shown in Figure 5 below. As expected, the LED1 peak adds to the LED2 peak to approximately equal the peak for both LEDs. This additive characteristic was checked using the normalization results from the fit for each LED, and for voltages below approximately 8.0V, the normalization results from LEDs 1 and 2 added to equal the results of both LEDs flashing at the same time.

To detect light intensity in the low photon range, data is taken at a variety of volt-

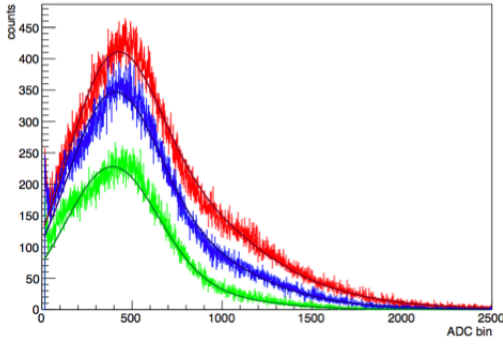


Figure 5: Results of fit for LED1 flashing at 6.8V shown in blue, and LED2 flashing at 6.5V shown in green. The results of both flashing at the same time are shown in red.

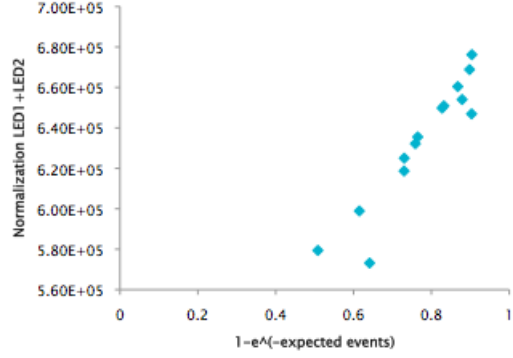


Figure 6: Data collected for voltages between 5.6V and 7.5 V, plotted as number of counts observed versus probability of getting zero photons.

ages, each result is fit, and results from all voltages are graphically compared based on equation 10.

$$N_{obs} = N_{exp}(1 - e^{-\lambda}) \quad (10)$$

This equation describes the relationship between the number of photons expected and the number observed. Collecting data at such low intensities, there is some probability of getting zero photons, which is the case where $k=0$ in equation 10. Therefore the number of photons observed is the number expected minus the probability of zero photons. Knowing the number of counts observed (the normalization result of the fit) and calculating the probability of zero gives the number of photons expected. For multiple fit results, plotting the number of counts observed versus the probability of getting zero photons should give a linear trend. Shown in Figure 6, the graph does have a linear trend as expected, and the number of expected events can be calculated for each data set.

3.2 Discussion

The data taken for LEDs 1 and 2 being pulsed at varying voltages was fit to the single photon peak, and at higher voltages, fit to multiple photon peaks, which should be able to be applied as the new unit of light yield instead of the arbitrary ADC count used by Reference [3]. However, there were limitations in the electronic setup of the experiment which restricted the power supply to no more than 8.0V. Since a preamplifier, amplifier, delay module, and second amplifier were all used in the electronic setup, the electronic noise was great enough that it obscured the signal if the power supply was above 8.0V, and the photon fit could not be applied. Changing the electronics setup by using a TTL to NIM converter instead of a chain of electronics should fine tune the signal so that higher voltages can be reached without noise dominating the signal. Once a wider range of voltages can be applied, fit results will include clearer single and multiple photon peaks, which will then be extended to the data from Reference [3] to represent light yield in terms of photons,

rather than the current results represented in arbitrary units of ADC counts.

4 Conclusion

This research resulted in a more extensive understanding of the behavior of particles in the SNO+ experiment. By collecting scattering data for different scintillator samples at a variety of wavelengths, angles, and polarizations, and fitting it to a Rayleigh scattering function, the scattering lengths of photons in different scintillator materials was determined. The results show that 0.3%Nd doped scintillator gives long enough scattering lengths such that the time dependency of detected photons is predictable, while for 0.3%Te doped scintillator, the scattering length is too short for this to be the case.

Data collected for light yield as a function of electron energy was also fit using a function for single and multiple photons peaks. The results, although limited by the electronics setup, show a linear trend corresponding to the number of expected photons. This data, in addition to higher voltage data will be used to calibrate the units of light yield results from Reference [3] based on a single photon scale.

5 Acknowledgements

I would like to thank Dr. Nikolai Tolich for being an excellent mentor and teacher. I would also like to thank Tim Major for introducing me to the lab and giving guidance throughout the project. Thank you also to Dr. Gupta and Dr. Garcia as well as Janine Nemerever and Linda Vilett for running the REU program.

I am also very grateful to the National

Science Foundation for providing funding for this research project.

6 References

- [1] M.C. Chen, The SNO+ Experiment, proceedings of the 34th International Conference on High Energy Physics (ICHEP 2008), Philadelphia, Pennsylvania (2008). arXiv:0810.369
- [2] V. Lozza et al., Scintillator Phase of the SNO+ Experiment (2012). arXiv:1201.6599
- [3] H. Wan Chan Tseung, J. Kaspar, N. Tolich, Measurement of the dependence of the light yields of linear alkylbenzene-based and EJ-301 scintillators on electron energy (2011). arXiv:1105.2100
- [4] A. Kokhanovsky, Optics of Light Scattering Media (Praxis Publishing, Chichester, England, 1999) pp. 23-24.
- [5] W.R. Leo, Techniques for Nuclear and Particle Physics Experiments: A How-to Approach (Springer-Verlag, Berlin Heidelberg 1987) pp. 79-82.